

Elemental 2-D mapping and changes in leaf iron and chlorophyll in response to iron re-supply in iron-deficient GF 677 peach-almond hybrid.

S. Jiménez^{1*}, F. Morales^{2*}, A. Abadía², J. Abadía², M.A. Moreno¹ and Y. Gogorcena¹
Departments of Pomology¹ and Plant Nutrition², Aula Dei Experimental Station,
Consejo Superior de Investigaciones Científicas (CSIC), Apdo. 13034, E-50080
Zaragoza, Spain

*Both authors contributed equally to this work

Author for correspondence:

Yolanda Gogorcena

Tel: +34 976 716133

FAX: +34 976 716145

Email: aoiz@eead.csic.es

Number of text pages: 21

Number of Figures: 8

Number of Tables: 2

Abstract

Iron is an essential micronutrient for plant growth and development, involved in key cellular processes. However, the distribution of Fe in plant tissues is still not well known. In the so-called Fe chlorosis paradox, leaves of fruit trees grown in the field usually have high concentrations of Fe but still are Fe-deficient. Leaves of the *Prunus* rootstock GF 677 (*P. dulcis* x *P. persica*) grown in hydroponics have been used to carry out two-dimensional (2-D) nutrient mapping by synchrotron radiation-induced X-ray fluorescence. Iron-deficient leaves accumulated more Fe in the midrib and veins, with Fe concentration being markedly lower in mesophyll leaf areas. The effects of Fe deficiency and Fe re-supply on leaf chlorophyll concentration and on the distribution of Fe and other nutrients within different plant tissues have been investigated in the same plants. After Fe re-supply, leaf Fe concentrations increased largely in all leaf types. However, whereas re-greening was almost completely achieved in apical leaves in some expanded leaves the increase in chlorophyll concentration was only moderate. Therefore, after Fe re-supply Fe-deficient expanded leaves of the *Prunus* rootstock GF 677 had significant increases in Fe concentration but were still chlorotic. This is similar to what occurs in leaves of peach trees in field conditions, opening the possibility that this system could be used as a model to study the Fe chlorosis paradox.

Keywords: inactive iron, iron chlorosis, iron deficiency, iron re-supply, leaf iron distribution, *Prunus*.

Abbreviations: Chl, chlorophyll; EDTA, ethylenediaminetetracetic acid; DW, dry weight; μ -SRXF, synchrotron radiation-induced X-ray fluorescence.

44 **Introduction**

45 Iron deficiency is one of the major abiotic stresses affecting fruit tree crops
46 growing in calcareous soils in the Mediterranean area. The most obvious effect of Fe
47 deficiency is the yellowing of young leaves, and therefore Fe deficiency is usually
48 referred to as Fe chlorosis. Peach is one of the fruit tree crops most affected by Fe
49 chlorosis, and growers not using appropriate rootstocks and/or Fe fertilization face
50 major losses in crop yield and quality (see review by Álvarez-Fernández et al.
51 2006), as well as marked reductions in orchard longevity (Sanz et al. 1992).

52 In plants, Fe is currently thought to be mobile within the root symplast chelated
53 with nicotianamine (NA) (Hell and Stephan 2003, Kim and Guerinot 2007). Then, it
54 is generally agreed that Fe is released into xylem vessels, and transported as
55 Fe(III)-citrate complexes (Hell and Stephan 2003), possibly in species such as [Fe-
56 CitrateOH]⁻¹ and [Fe-Citrate₂]⁻³ (López-Millán et al. 2000). Iron is thought to be
57 taken up into the leaf symplast by a system including a ferric chelate reductase
58 (González-Vallejo et al. 2000; Larbi et al. 2001; Mukherjee et al. 2006), to be
59 chelated again by NA in the cell (Hell and Stephan 2003; Takahashi et al. 2003).
60 Mobility of Fe from source to sink tissues in plants is still poorly documented (Curie
61 and Briat 2003), but Fe is thought to be mobile to some extent in the phloem
62 (Krüger et al. 2002; Hüve et al. 2003; Andaluz 2005).

63 The peach rootstock GF 677 (*P. dulcis* x *P. persica*) is widely used in the
64 Mediterranean area (Jiménez et al. 2008, and references therein). Previous studies
65 have characterized the leaf nutrient composition (Gogorcena et al. 2004) and
66 agronomical performance of this genotype (Iglesias et al. 2004; Zarrouk et al.
67 2005). When grown under Fe deficiency, the roots of this rootstock show increased
68 proton extrusion (Molassiotis et al. 2006) and Fe-reduction rates (Romera et al.
69 1991a, 1991b; Cinelli et al. 2004). However, the elicitation of root Fe reductase
70 activity upon Fe deficiency requires in this genotype the presence of some Fe in the
71 nutrient solution (Gogorcena et al. 2004).

In spite of the efforts in Fe research in the last decades, the distribution and roles of Fe in plant organs are still not fully known, especially in woody species. The most common technique used to assess the degree of Fe deficiency-chlorosis is the measurement of total Fe concentration in leaves, with leaf Fe concentrations required for optimal growth being usually in the range of 50 to 150 mg kg⁻¹ dry mass (DW) (Marschner 1991). In many cases, however, leaves from Fe-deficient plants grown in the field have quite high leaf Fe concentrations (>80-100 mg Fe kg⁻¹ DW), and there is no good correlation between leaf Fe and Chl concentrations (Morales et al. 1998, and references therein). This has been termed the "Fe-chlorosis paradox" (Morales et al. 1998; Römheld 2000), and suggests that part of the Fe acquired from the soil by Fe-deficient plants could be immobilized and accumulated in inactive forms somewhere in the leaf (Morales et al. 1998).

Knowledge on the spatial distribution of nutrients in plant tissues can be gained using combinations of image and spectroscopic techniques. For instance, mapping metals in woody plant tissues has been done using synchrotron radiation-induced X-ray fluorescence (μ -SRXF) and scanning electron microscopy with energy dispersive X-ray microanalysis (SEM-EDX) (Marmioli et al. 1999). Iron distribution in different plant organs has been studied using several techniques, including EDX (Kosegarten and Koyro 2001), electron spectroscopic imaging (ESI) (Liu et al. 1998) and reflection X-ray fluorescence spectrometry (TXRF), either alone (Fodor et al. 2005) or in combination with EDX (Rodríguez et al. 2005). Two-dimensional μ -SRXF imaging of metal (including Fe) distribution has been carried out in different plant tissues (McNear et al. 2005; Punshon et al. 2005; Isaure et al. 2006). Also, 3-D μ -SRXF micro-tomography has been used to study Fe localization in seeds (Kim et al. 2006). Other techniques such as nuclear magnetic resonance imaging (MRI; Lambert et al. 2006) and positron-emitting tracer imaging (PETIS; Ishimaru et al. 2006) have been only recently used.

The aim of this work was to investigate the effects of Fe re-supply on the changes in Fe and chlorophyll concentrations in different leaf types in the GF 677

peach-almond hybrid grown in hydroponics. Also, the leaf nutrient 2-D distribution (in midrib, veins and interveinal mesophyll areas) was assessed in Fe-deficient and Fe-sufficient GF 677 by μ -SRXF.

Materials and methods

Plant material and culture

Micropropagated GF 677 rootstock plants [*Prunus dulcis* (Mill.) D.A. Webb x *Prunus persica* (L.) Batsch] were obtained from Agromillora Catalana S.A. (Subirats, Barcelona, Spain). Plants were grown for two weeks in 300 mL pots containing a peat substrate.

The protocol to obtain Fe-deficient plants is shown in Figure 1a. Plants were transferred to 10 L plastic boxes (30 plants per container) filled with a continuously aerated, half-strength Hoagland solution, containing (in mM) 2.5 $\text{Ca}(\text{NO}_3)_2$, 2.5 KNO_3 , 1 MgSO_4 , 1 KH_2PO_4 , and (in μM) 46.2 H_3BO_3 , 9.2 MnCl_2 , 0.38 CuSO_4 , 2.4 ZnSO_4 , and 0.12 Na_2MoO_4 , pH 6.0. Solutions also contained 90 μM Fe(III)-EDTA. Plants were grown in a growth chamber with a photoperiod of 16 h light (220-250 $\mu\text{mol photon m}^{-2} \text{s}^{-1}$ at the leaf level) at 23°C/8 h of darkness at 20°C, and 70-75% relative humidity. The pH of the nutrient solution was adjusted to 6.0 daily using 1 N HCl. Nutrient solutions were changed every week.

After 2 weeks of growth, when roots were about 10 cm long, plants were transferred to boxes containing 0 μM [-Fe] or 90 μM Fe(III)-EDTA [+Fe] (in both cases 10 L boxes, approximately 30 plants per box) (Fig. 1A). After 14 days without Fe, [-Fe] plants were re-supplied with 180 μM Fe(III)-EDTA [180Fe] in boxes that had previously no Fe (the day of the Fe re-supply was named d 0) (Fig. 1a). Plants were grown under these conditions for 7 additional days, and during this period the re-supply nutrient solution [180Fe] was renewed every two days, to maintain an Fe concentration as constant as possible. In the [-Fe] and [+Fe] treatments solutions were renewed every four days. The 180 μM Fe(III)-EDTA concentration was chosen

to maximize Fe uptake, considering an early study where it was found that the elicitation of FC-R activity after 1 day was larger with 180 than with 45 μM Fe (Gogorcena et al. 2000). This Fe concentration was not toxic to plants, since they did not show any leaf or root toxicity symptoms, and showed growth rates similar to those of controls in experiments lasting several weeks (not shown).

At d 0, leaves of all plants were labeled with tape: expanded leaves were marked 1 to 4, whereas basal leaves were marked 5 to 11. Apical leaves were those leaves developed and expanded during the experiments, and were named 0 to -4 (Fig. 1b; in this figure only three apical leaves, 0, -1 and -2, are depicted).

Growth was determined by measuring the fresh weight (FW) of the root and shoot of every plant in all treatments.

Two-dimensional elemental leaf distribution

The 2-D element distribution (mapping) of first expanded leaves of [+Fe] and [-Fe] plants was determined by $\mu\text{-SRXF}$. Analyses were carried out at beam line D15 (DCI, LURE, Orsay, France), with a 100- μm beam of 10 keV. Two-dimensional mapping was carried out by step-wise scanning of the sample, with a counting time of 1 and 2 min in [+Fe] and [-Fe], respectively. Elements were mapped taking into account this difference in counting time. Data were not normalized to the intensity of the incident X-ray beam, which decreased routinely by approximately 3-7% during the scanning time (usually several hours). The resolution of the probe was approximately 100 μm , and the analysis corresponded to the full depth (thickness) of the leaf.

First expanded leaves were taken from 5-weeks old [+Fe] and [-Fe] plants at d 7. Leaves of [+Fe] plants had approximately 285 μmol chlorophyll (Chl) m^{-2} and 267 mg Fe kg^{-1} DW, whereas those of [-Fe] plants had approximately 28 μmol Chl m^{-2} and 155 mg Fe kg^{-1} DW (Fig. 2). Leaves were washed, dried on absorbent paper, and square leaf pieces, approximately 3 x 3 mm, including midrib, veins and interveinal spaces (Fig. 2) were scanned for macro- (Ca, K, and S) and micro-

nutrients (Fe, Mn, Zn, Cu, and Cl). Traces of other elements, such as Cr, V and Ti, were also observed (data not shown).

Leaf chlorophyll determination

Leaf chlorophyll was monitored daily in 4 plants per treatment, using a SPAD 502 meter (Minolta Co., Osaka, Japan). Six SPAD measurements per leaf, homogeneously distributed from the apex to the base of the leaf, were taken and averaged to obtain a representative Chl concentration value. For calibration, leaf disks with different degrees of Fe deficiency were first measured with the SPAD and then extracted with 100% (v/v) acetone in the presence of Na ascorbate. Chlorophyll was measured spectrophotometrically according to Abadía and Abadía (1993). The relationship between SPAD values and Chl concentration (in $\mu\text{mol m}^{-2}$) was $\text{Chl} = 0.127 \text{ SPAD}^2 + 0.694 \text{ SPAD} + 16.909$ ($R^2 = 0.99$) (data not shown).

Iron analysis

Iron concentrations were measured in apical (0 to -4 in the controls, 0 to -3 in the [180Fe] and 0 to -2 in the [-Fe]), expanded (1 to 4) and basal leaves (5 to 11), stems and roots (Fig. 1b). Samples were run in 3 replicates, except for apical leaves, which had a very low mass and were pooled in a single sample.

Samples were washed with 0.1 M HCl to eliminate contamination from the nutrient solution, and then rinsed three times with ultrapure water. In the case of leaves the midrib was removed. Then, samples were dried in a forced air oven at 60 °C during 48 h, ground to powder, dry-ashed and the residue dissolved in HNO₃ and HCl following standard procedures (A.O.A.C. 1990). Iron was determined by flame AAS (Unicam-969 AA spectrometer).

Measurement of *in vivo* root Fe(III)-EDTA reduction with intact plants

Plant roots were thoroughly rinsed in de-ionized water, and individual plants were transferred to 50 mL black plastic beakers, covered with tape to exclude light, containing 50 mL of 300 μM bathophenanthrolinedisulfonic acid (BPDS; ACROS

Organics) and 10 mM MES pH 6.0, as described in Gogorcena et al. (2000). The buffer solution was continually aerated by using plastic tubing. Once plants had been placed in the beakers, Fe(III)-EDTA (Sigma) was added to a final concentration of 500 μ M. After 1 h, 1 mL aliquots were taken and centrifuged. Reduction rates were estimated spectrophotometrically from the formation of the Fe(II)-BPDS₃ colored complex at 535 nm from Fe(III)-EDTA (Chaney et al. 1972; Bienfait et al. 1983), using an extinction coefficient of 22.14 mM⁻¹ cm⁻¹. Blank measurements without plants were also carried out.

Root FC-R activity was measured at d 0, d 3 and d 7 for [+Fe], d 0, d 4 and d 7 for [-Fe], and daily from d 1 to 7 for [¹⁸⁰Fe], with 4 replicates per treatment. Plants used for FC-R measurements were also used for Fe analysis and growth measurements.

Statistical analysis

Data were evaluated by analysis of variance with SPSS 13.0.1 (SPSS, Inc, Chicago, USA). When the F test was significant, means were separated by Duncan's Multiple Range test ($P \leq 0.05$). Regression analysis was carried out by Pearson's correlation analysis.

Results

Plant growth

After 14 days without Fe (at d 0), shoot growth was significantly inhibited by Fe deficiency, whereas root growth was unaffected when compared with that of control plants (Table 1). The fresh weight of [-Fe] leaves was reduced especially in apical leaves, where it was less than 20% of that of [+Fe] leaves (data not shown). After 21 d of imposing Fe deficiency (at d 7), shoot growth was significantly inhibited by Fe deficiency, whereas root growth was still not significantly affected (Table 1). At this stage, five (leaves 0 to -4) and four (leaves 0 to -3) new apical leaves had expanded in [+Fe] and [¹⁸⁰Fe] plants, respectively, whereas only two new leaves

(leaves 0 and -1) had appeared in the [-Fe] plants. The Fe re-supply induced very little growth in the Fe-deficient plants during the 7 days of the experiment (Table 1). However, in the long term (several weeks) Fe-resupplied plants grew very well, with growth rates comparable to those of Fe-sufficient controls (data not shown).

Leaf nutrient distribution

The 2-dimensional element distribution showed remarkable differences between [+Fe] and [-Fe] leaves. Typical elemental maps in both types of leaves are shown in Figs. 3 and 4. Major differences occurred in nutrient concentrations, and in their distribution among midrib, veins and interveinal mesophyll areas.

Under [+Fe] conditions, Fe was preferentially located in the midrib, and no differences were found between veins and interveinal areas (Fig. 3). Iron co-localized with Mn, Zn, Cu, and Ca (Table 2; Figs. 3 and 4). Potassium and Cl were preferentially located in the midrib and veins, whereas S was distributed homogeneously (Fig. 4).

Under [-Fe] conditions, Fe concentrations were low in all leaf parts, and especially in interveinal areas (Fig. 3). The Mn, Zn and Cu signals were higher in [-Fe] plants than in the Fe-sufficient controls. Fe co-localized with Mn, Zn, and Ca, but not with Cu (Table 2; Figs. 3 and 4). Copper was preferentially located in the midrib (Fig. 3), whereas the distribution of K, Cl and S was fairly homogeneous (Fig. 4). The lack of significant co-localization of Cu and Fe in [-Fe] conditions (Table 2) was due to the low Cu signals in veins (Fig. 3), and the reason for this is not known. Also, the basis for the differences in localization of K and Cl in [-Fe] and [+Fe] conditions deserve further investigation, although in the case of K it may be related to the known increases in leaf K concentration with Fe deficiency.

Leaf chlorophyll concentration

Four different groups of leaves can be distinguished when looking at the Chl concentrations of the [-Fe], [+Fe] and [180Fe] plants after 7 days of Fe re-supply

(Fig. 5). The first group included apical leaves (leaves 0 to -4), which had re-greened almost completely 7 days after Fe-re-supply; in leaves 0 to -3 differences in Chl concentration between [+Fe] and [180Fe] plants were not significant (data not shown). In a second group of leaves, which included young leaves already expanded at the start of the treatment (leaves 1 to 4) the Chl values in the [180Fe] treatment did not reach those found in the [+Fe] controls (this group is enclosed in a box in Fig. 5). A third group of leaves (leaves 5 to 7) was only moderately chlorotic at the start of the treatment and Chl did not increase significantly thereafter, whereas a fourth group corresponding to the most basal, older leaves (leaves 8 to 11) was always green in all treatments.

Iron concentrations of different plant parts

In leaves, Fe concentrations increased after Fe re-supply until days 3-4 (Fig. 6) to decrease slightly thereafter. At d 3-4, the leaf Fe concentration of [180Fe] plants was in the range 350-650 mg Fe kg⁻¹ DW, more than two-fold higher than those found in the [+Fe] and [-Fe] plants (50-230 mg Fe kg⁻¹ DW). Apical, expanded and basal leaves had similar Fe concentrations during the experiment for a given treatment.

Roots of Fe-deficient plants had Fe concentrations of approximately 400 mg kg⁻¹ DW, lower than those found in the Fe-sufficient controls (Fig. 6). However, only 1 day after re-supply Fe concentrations in roots were approximately 2,000 mg Fe kg⁻¹ DW, and similar concentrations were also found in the following days. It should be taken into account that the acid procedure used to wash roots is unlikely to remove all Fe that could precipitate in the root apoplast of plants grown in hydroponics with Fe-chelates (e.g., 75% of the total Fe in dry bean, Bienfait et al. 1985, and 84% in poplar, Fodor et al. 2005). In the stems the re-supply treatment did not lead to Fe concentrations above 170 mg Fe kg⁻¹ DW, values not much higher than those found in the controls.

Relationships between Fe and chlorophyll concentrations during Fe re-supply

When looking at Fe and Chl leaf concentration values, basal leaves were found to behave differently to expanded and apical leaves during Fe re-supply (Fig. 7). In basal leaves the mean Chl concentration remained fairly constant (not significant differences were found at $P \leq 0.05$), whereas the mean Fe concentrations increased significantly (at $P \leq 0.001$). Expanded leaves, however, responded first with increases in both Chl and Fe concentrations, followed by further increases in Chl that were accompanied by decreases in Fe ($P \leq 0.01$). Apical leaves responded similarly to expanded leaves, although no statistical significances can be inferred due to lack of replicates.

Root ferric chelate-reductase (FC-R) activity

The FC-R activity of Fe-sufficient plants was in the range 5-8 nmol Fe(II) g⁻¹ FW min⁻¹, whereas those of Fe-deficient plants were lower than 1 nmol Fe(II) g⁻¹ FW min⁻¹ (Fig. 8). This is in agreement with previous reports indicating that the elicitation of FC-R activity in Fe-deficient *Prunus* spp. require the presence of some Fe in the nutrient solution (Gogorcena et al. 2000; 2004). After 1 day of Fe re-supply, the FC-R rates increased to approximately 14 nmol Fe(II) g⁻¹ FW min⁻¹ (Fig. 8). On days 2 to 4, the FC-R activities of [180Fe] plants decreased to approximately 10 nmol Fe(II) g⁻¹ FW min⁻¹, and on days 5 to 7 rates were lower than those found in [+Fe] plants. Therefore, on day 1 after re-supply the FC-R activity of [180Fe] plants was approximately 2.5-fold higher than that of [+Fe] plants, and approximately 13.5-fold higher than [-Fe] plants before Fe re-supply.

Discussion

Measuring total leaf Fe concentration is one of the most common techniques used to assess the degree of Fe chlorosis. This approach, however, presents major problems, since in many cases when leaves from field-grown, Fe-chlorotic plants are analyzed, leaf Fe concentrations are relatively high ($>80\text{--}100\text{ mg Fe kg}^{-1}$ dry mass). These Fe concentrations do not correlate with leaf Chl, and this has been called the “Fe-chlorosis paradox” (Morales et al. 1998; Römheld 2000). Iron deficiency has been reported to decrease shoot growth in several species, including grapevine (Gruber and Kosegarten 2002; Jiménez et al. 2007), peach (Shi et al. 1993; Alcántara et al. 2000) and the GF 677 peach x almond hybrid (this work), and Fe deficiency may prevent nuclear and cellular division by inhibiting key metabolic enzymes such as ribonucleotide reductase (Kosegarten and Koyro 2001) and impair meristematic growth (Mengel 1994). Reductions in leaf growth would produce apparently high Fe concentrations, when expressed on a dry matter basis (Römheld 2000).

The “iron chlorosis paradox” could be associated to a tissue-specific Fe location (Römheld 2000). Iron localization, assessed by synchrotron radiation-induced X-ray fluorescence, indicate that in chlorotic leaves Fe is preferentially located in midribs and veins, with interveinal mesophyll areas having low Fe. Iron-sufficient leaves had similar Fe concentrations in veins and interveinal mesophyll areas, with high Fe concentrations being found in midribs. Leaf mineral analyses are usually carried out after midrib removal, and a large part of the total leaf Fe is located in this tissue, both in Fe-sufficient and Fe-deficient leaves. Using for analyses chlorotic leaves where the midrib has been removed would still produce somewhat high Fe concentrations, because vein areas in these leaves could have high Fe. To observe a more marked difference in Fe concentration between chlorotic and Fe-sufficient leaves leaf mineral analysis should be carried out with interveinal mesophyll areas. These differences of Fe distribution between chlorotic and Fe-sufficient leaves may

also explain why chlorosis is often interveinal, with Fe and Chl co-localizing in areas close to the midrib and veins.

The accumulation of divalent metal cations under Fe deficiency conditions may be related to the lack of specificity of transporters and the FC-R, since both proteins may use other metals in addition to Fe (Reid 2001; Chen et al. 2004; Kim and Guerinot 2007). Leaf P increased with Fe chlorosis (Jiménez 2006), and this might indicate that the accumulated Fe could be precipitated as insoluble Fe-phosphate or other Fe- and P-containing compound such as phytate. In seeds and roots, K, Mg, Cu, Zn, Fe and Ca are stored in association with phytate (Becker et al. 1995, and references therein), and in rice grain P, Fe, Zn, Cu and Mn concentrations also correlate with phytate (Stangoulis et al. 2007). In Fe-deficient leaves all these elements co-localize (Table 2) and also increase their concentrations, with the exception of Fe (Figs. 3 and 4, and Jiménez 2006). The presence of phytate or another Fe phosphate compound in the midrib and veins of chlorotic leaves has not been investigated so far. The nature of physiologically inactive Fe pools is a matter that deserves further investigation.

There are some biochemical and physiological reasons by which the entrance of Fe from midribs and veins to leaf limb cells may be hampered. These include an impairment of the Fe(III)-chelate reductase enzyme needed to reduce Fe(III) to Fe(II) before it enters leaf cells. Possible causes include an intrinsic decrease in Fe(III)-chelate reductase enzyme activity (González-Vallejo et al. 2000; Larbi et al. 2001), a possible shift in the apoplastic pH (González-Vallejo et al. 2000; López-Millán et al. 2001; Nikolic and Römheld 2003) and an accumulation of organic acids in the apoplastic space (López-Millán et al. 2000, and references therein). Also, the Fe(II) transporter needed in leaves could be inhibited in Fe-deficient leaves. All of these reasons could lead to the accumulation of physiologically inactive Fe pools in the apoplast of chlorotic leaves.

Growing plants under Fe deficiency conditions for some time and then re-supplying Fe in controlled growth chambers could be a good method to mimic the "Fe chlorosis paradox" in laboratory conditions. After two weeks of Fe deficiency, there was a gradient of leaf Chl concentrations from fully yellow apical youngest leaves, through expanded leaves with typical interveinal Fe chlorosis symptoms, and then to basal leaves, including some leaves (leaves 5 to 7) slightly affected by Fe deficiency and other (leaves 8 to 11) fully green. Apical leaves became green quickly after Fe re-supply, whereas fully chlorotic leaves re-greened very fast (data not shown). However, expanded leaves having a mild chlorosis did not regreen completely, confirming previous results of Alcántara et al. (2000). Upon Fe re-supply, all leaf types had large increases in Fe concentrations. Therefore, some leaves were still chlorotic but had high Fe concentrations (mimicking the "Fe chlorosis paradox"). Lack of re-greening of expanded leaves upon Fe re-supply could be explained by difficulties in recovering damaged structures or in using newly acquired Fe in cells (Bohórquez et al. 2001).

In conclusion, Fe was located preferentially in the midrib and veins in Fe-deficient leaves, and this could explain why chlorosis is often interveinal in field-grown chlorotic materials. This could be among the causes leading to the appearance of the "Fe chlorosis paradox". Growing plants under Fe deficiency conditions for some time and then re-supplying Fe could be a good method to mimic the "Fe chlorosis paradox" in controlled growth chambers, to better explain how plants transport Fe in different plant tissues.

Acknowledgements

Supported by grants from the Spanish MEC (AGL2005-05533 and AGL2006-1416) co-financed by FEDER, PETRI (PTR1995-0580) and DGA (A44 and A03). S. Jiménez was supported by an I3P-CSIC predoctoral fellowship (cofinanced by FSE). We gratefully acknowledge P. Chevallier and E. Foy for their help during the work with

368 μ -SRXF, R. Giménez for her help with figures and A. F. López-Millán and A. Álvarez-
369 Fernández for valuable discussion.

References

- Abadía J, Abadía A (1993) Iron and plant pigments. In: Barton LL, Hemming BC (eds) Iron Chelation in Plants and Soil Microorganisms. Academic Press, San Diego, pp 327-343
- Alcántara E, Romera FJ, Cañete M, de la Guardia MD (2000) Effects of bicarbonate and iron supply on Fe(III) reducing capacity of roots and leaf chlorosis of the susceptible peach rootstock "Nemaguard". J Plant Nutr 23:1607-1617
- Álvarez-Fernández A, Abadía J, Abadía A (2006) Iron deficiency, fruit yield and fruit quality. In: Barton LL, Abadía J (eds) Iron Nutrition in Plants and Rhizospheric Microorganisms. Springer, Dordrecht, pp 85-101
- Andaluz S (2005) Estudio de los cambios inducidos por la deficiencia de hierro en el proteoma de las plantas. PhD thesis. University of Zaragoza, Zaragoza
- A.O.A.C. (1990) Official Methods of Analysis of the Association of Official Analytical Chemists. Hedrich K (ed) Academic Press, Washington DC, pp 1141
- Becker R, Fritz E, Manteuffel R (1995) Subcellular localization and characterization of excessive iron in the nicotianamine-less tomato mutant *chloronerva*. Plant Physiol 108:269-275
- Bienfait HF, Bino RJ, van der Blik AM, Duivenvoorden JF, Fontaine JM (1983) Characterization of ferric reducing activity in roots of Fe-deficient *Phaseolus vulgaris*. Physiol Plantarum 59:196-202
- Bienfait HF, Van der Briel W, Mesland-Mul NT (1985) Free space iron pools in roots. Generation and mobilization. Plant Physiol 78:596-600
- Bohórquez JM, Romera FJ, Alcántara E (2001) Effect of Fe^{3+} , Zn^{2+} and Mn^{2+} on ferric reducing capacity and regreening process of the peach rootstock Nemaguard (*Prunus persica* (L.) Batsch). Plant Soil 237:157-163
- Chaney RL, Brown JC, Tiffin LO (1972) Obligatory reduction of ferric chelates in iron uptake by soybeans. Plant Physiol 50:208-213
- Chen Y, Shi J, Tian G, Zheng S, Lin Q (2004) Fe deficiency induces Cu uptake and accumulation in *Commelina communis*. Plant Sci 166:1371-1377

399 Cinelli F, Tamantini I, Iacona C (2004) Nutritional (Fe-Mn) interactions in 'Big Top'
400 peach plants as influenced by the rootstock and by the soil CaCO_3
401 concentration. *Soil Sci Plant Nutr* 50:1097-1102

402 Curie C, Briat J-F (2003) Iron transport and signaling in plants. *Annu Rev Plant Biol*
403 54:183-206

404 Fodor F, Gáspár L, Morales F, Gogorcena Y, Lucena JJ, Cseh E, Kröpfl K, Abadía J,
405 Sárvári É (2005) Effects of two iron sources on iron and cadmium allocation in
406 poplar (*Populus alba*) plants exposed to cadmium. *Tree Physiol* 25:1173-1180

407 Gogorcena Y, Abadía J, Abadía A (2000) Induction of *in vivo* root ferric chelate
408 reductase activity in fruit tree rootstock. *J Plant Nutr* 23:9-21

409 Gogorcena Y, Abadía J, Abadía A (2004) A new technique for screening iron-
410 efficient genotypes in peach rootstocks: elicitation of root ferric chelate
411 reductase by manipulation of external iron concentrations. *J Plant Nutr*
412 27:1701-1715

413 González-Vallejo EB, Morales F, Cistué L, Abadía A, Abadía J (2000) Iron deficiency
414 decreases the Fe(III)-chelate reducing activity of leaf protoplasts. *Plant Physiol*
415 122:337-344

416 Gruber B, Kosegarten H (2002) Depressed growth of non-chlorotic vine grown in
417 calcareous soil is an iron deficiency symptom prior to leaf chlorosis. *J Plant Nutr*
418 25:111-117

419 Hell R, Stephan UW (2003) Iron uptake, trafficking and homeostasis in plants.
420 *Planta* 216:541-551.

421 Hüve K, Remus R, Lüttschwager D, Merbach W (2003) Transport of foliar applied
422 iron (^{59}Fe) in *Vicia faba*. *J Plant Nutr* 26:2231-2242

423 Iglesias I, Monserrat R, Carbó J, Bonany J, Casals M (2004) Evaluation of
424 agronomical performance of several peach rootstocks in Lleida and Girona
425 (Catalonia, NE-Spain). *Acta Hort* 658:341-348

426 Isaure M-P, Frayssé A, Devès G, le Lay P, Fayard B, Susini J, Bourguignon J, Ortega
427 R (2006) Micro-chemical imaging of cesium distribution in *Arabidopsis thaliana*

428 plant and its interaction with potassium and essential trace elements. *Biochimie*
429 88:1583-1590

430 Ishimaru Y, Suzuki M, Tsukamoto T, Suzuki K, Nakazono M, Kobayashi T, Wada Y,
431 Watanabe S, Matsushashi S, Takahashi M, Nakanishi H, Mori S, Nishizawa NK
432 (2006) Rice plants take up iron as an Fe^{3+} -phytosiderophore and as Fe^{2+} . *Plant J*
433 45:335-346

434 Jiménez S (2006) Selección de patrones frutales de hueso tolerantes a la clorosis
435 férrica. Aspectos nutricionales y metabólicos. PhD thesis, University of
436 Zaragoza, Zaragoza

437 Jiménez S, Gogorcena Y, Hevin C, Rombolà AD, Ollat N (2007) Nitrogen nutrition
438 influences some biochemical responses to iron deficiency in tolerant and
439 sensitive genotypes of *Vitis*. *Plant Soil* 290:343-355

440 Jiménez S, Pinochet J, Abadía A, Moreno MA, Gogorcena Y (2008) Tolerance
441 response to iron chlorosis of *Prunus* selections as rootstocks. *HortScience*
442 43:304-309

443 Kim SA, Guerinot ML (2007) Mining iron: Iron uptake and transport in plants. *FEBS*
444 Lett 581:2273-2280

445 Kim SA, Punshon T, Lanzirotti A, Li L, Alonso JM, Ecker JR, Kaplan J, Guerinot ML
446 (2006) Localization of iron in *Arabidopsis* seed requires the vacuolar membrane
447 transporter VIT1. *Science* 314:1295-1298

448 Kosegarten H, Koyro H-W (2001) Apoplastic accumulation of iron in the epidermis
449 of maize (*Zea mays*) roots grown in calcareous soil. *Physiol Plantarum* 113:515-
450 522

451 Krüger C, Berkowitz O, Stephan UW, Hell R (2002) A metal-binding member of the
452 late embryogenesis abundant protein family transports iron in the phloem of
453 *Ricinus communis* L. *J Biol Chem* 277:25062-25069

454 Lambert J, Lampen P, von Bohlen A, Hergenröder R (2006) Two- and three-
455 dimensional mapping of the iron distribution in the apoplasmic fluid of plant leaf
456 tissue by means of magnetic resonance imaging. *Anal Bioanal Chem* 384:231-

- Larbi A, Morales F, López-Millán AF, Gogorcena Y, Abadía A, Moog PR, Abadía J (2001) Technical advance: Reduction of Fe(III)-chelates by mesophyll leaf disks of sugar beet. Multi-component origin and effects of Fe deficiency. *Plant Cell Physiol* 42:94-105
- Liu DH, Adler K, Stephan UW (1998) Iron-containing particles accumulate in organelles and vacuoles of leaf and root cells in the nicotianamine-free tomato mutant *chloronerva*. *Protoplasma* 201:213-220
- López-Millán A-F, Morales F, Abadía A, Abadía J (2000) Effects of iron deficiency on the composition of the leaf apoplastic fluid and xylem sap in sugar beet. Implications for iron and carbon transport. *Plant Physiol* 124:873-884
- López-Millán AF, Morales F, Abadía A, Abadía J (2001) Iron deficiency-associated changes in the composition of the leaf apoplastic fluid from field-grown pear (*Pyrus communis* L.) trees. *J Exp Bot* 52:1489-1498
- Marmiroli N, Maestri E, Antonioli G, Conte C, Mociardini P, Marmiroli M, Mucchino C (1999) Application of synchrotron radiation X-ray fluorescence (μ -SRXF) and X-ray microanalysis (SEM/EDX) for the quantitative and qualitative evaluation of trace element accumulation in woody plants. *Int J Phytoremediat* 1:169-187
- Marschner H (1991) Symposium summary and future research areas. In: Chen Y, Hadar Y (eds) *Iron Nutrition and Interactions in Plants*. Kluwer Academic Publishers, Dordrecht, pp 365-372
- McNear Jr DH, Peltier E, Everhart J, Chaney RL, Sutton S, Newville M, Rivers M, Sparks DL (2005) Application of quantitative fluorescence and absorption-edge computed microtomography to image metal compartmentalization in *Alyssum murale*. *Environ Sci Technol* 39:2210-2218
- Mengel K (1994) Iron availability in plant tissues - iron chlorosis on calcareous soils. *Plant Soil* 165:275-283
- Molassiotis A, Tanou G, Diamantidis G, Patakas A, Therios I (2006) Effects of 4-month Fe deficiency exposure on Fe reduction mechanism, photosynthetic gas

486 exchange, chlorophyll fluorescence and antioxidant defense in two peach
 487 rootstocks differing in Fe deficiency tolerance. J Plant Physiol 163:176-185
 488 Morales F, Grasa R, Abadía A, Abadía J (1998) Iron chlorosis paradox in fruit trees.
 489 J Plant Nutr 21:815-825
 490 Mukherjee I, Campbell NH, Ash JS, Connolly EL (2006) Expression profiling of the
 491 *Arabidopsis* ferric chelate reductase (*FRO*) gene family reveals differential
 492 regulation by iron and copper. Planta 223:1178-1190
 493 Nikolic M, Römheld V (2003) Nitrate does not result in iron inactivation in the
 494 apoplast of sunflower leaves. Plant Physiol 132:1303-1314
 495 Punshon T, Lanzirotti A, Harper S, Bertsch PM, Burger J (2005) Distribution and
 496 speciation of metals in annual rings of black willow. J Environ Qual 34:1165-
 497 1173
 498 Reid RJ (2001) Mechanisms of micronutrient uptake in plants. Aust J Plant Physiol
 499 28:659-666
 500 Rodríguez N, Menéndez N, Tornero J, Amils R, de la Fuente V (2005) Internal iron
 501 biomineralization in *Imperata cylindrica*, a perennial grass: chemical
 502 composition, speciation and plant localization. New Phytol 165:781-789
 503 Romera FJ, Alcántara E, de la Guardia MD (1991a) Characterization of the tolerance
 504 to iron chlorosis in different peach rootstocks grown in nutrient solution. I.
 505 Effect of bicarbonate and phosphate. Plant Soil 130:115-119
 506 Romera FJ, Alcántara E, de la Guardia MD (1991b) Characterization of the tolerance
 507 to iron chlorosis in different peach rootstocks grown in nutrient solution. II.
 508 Iron-stress response mechanism. Plant Soil 130:121-125
 509 Römheld V (2000) The chlorosis paradox: Fe inactivation in leaves as a secondary
 510 event in Fe deficiency chlorosis. J Plant Nutr 23:1629-1643
 511 Sanz M, Caverio J, Abadía J (1992) Iron chlorosis in the Ebro river basin, Spain. J
 512 Plant Nutr 15:1971-1981
 513 Shi Y, Byrne DH, Reed DW, Loeppert RH (1993) Iron chlorosis development and
 514 growth response of peach rootstocks to bicarbonate. J Plant Nutr 16:1039-1046

515 Stangoulis JCR, Huynh B-L, Welch RM, Choi E-Y, Graham RD (2007) Quantitative
 516 trait loci for phytate in rice grain and their relationship with grain micronutrient
 517 content. *Euphytica* 154:289-294
 518 Takahashi M, Terada Y, Nakai I, Nakanishi H, Yoshimura E, Mori S, Nishizawa NK
 519 (2003) Role of nicotianamine in the intracellular delivery of metals and plant
 520 reproductive development. *Plant Cell* 15:1263-1280
 521 Zarrouk O, Gogorcena Y, Gómez-Aparisi J, Betrán JA, Moreno MA (2005) Influence
 522 of almond x peach hybrids rootstocks on flower and leaf mineral concentration,
 523 yield and vigour of two peach cultivars. *Sci Hortic* 106: 502-514

Tables

Table 1 Plant growth of GF 677 plants during the 7-d Fe re-supply experiment. Plants had been grown previously for 14 d with 90 μM Fe [+Fe] or 0 μM Fe [-Fe]. Fresh Weight (FW) was measured at days 0 and 7 in Fe-deficient plants growing with 0 μM Fe ([-Fe]), in Fe-sufficient plants growing with 90 μM Fe(III)-EDTA ([+Fe]) and in re-supplied plants growing with 180 μM Fe(III)-EDTA [180Fe]. At each time point, measurements were carried out in different plants.

Treatment	Day	Root fresh weight (g)		Shoot fresh weight (g)	
+Fe	0	0.85 ± 0.11	a	3.2 ± 0.2	b
	7	1.42 ± 0.03	b	6.0 ± 0.1	c
-Fe	0	0.74 ± 0.07	a	2.5 ± 0.2	a
	7	1.26 ± 0.19	b	3.6 ± 0.3	b
180Fe	0	0.74 ± 0.07	a	2.5 ± 0.2	a
	7	1.06 ± 0.12	ab	3.2 ± 0.3	b

Data are means \pm SE of 4 replicates. Means in the same column followed by the same letter were not significantly different, using Duncan's multiple range test at $P \leq 0.05$.

Table 2 Relationships between the concentrations of different elements in GF 677 leaves growing with 90 μM Fe(III)-EDTA [+Fe] and 0 μM Fe(III)-EDTA [-Fe]. Data were obtained from the elemental maps shown in Figs. 3 and 4, plotting synchrotron radiation-induced X-ray fluorescence ($\mu\text{-SRXF}$) values of each element *versus* the other. Each correlation was calculated with 900 data pairs (3 x 3 mm area, 100 μm resolution).

Treatment		Fe	Mn	Zn	Cu	Ca	K	Cl
[+Fe]	Mn	0.671**						
	Zn	0.559**	0.745**					
	Cu	0.589**	0.660**	0.696**				
	Ca	0.501**	0.830**	0.643**	0.530**			
	K	ns	0.591**	0.655**	ns	0.588**		
	Cl	ns	ns	ns	ns	ns	0.731**	
	S	ns	ns	ns	ns	ns	ns	ns
[-Fe]	Mn	0.773**						
	Zn	0.715**	0.702**					
	Cu	ns	ns	ns				
	Ca	0.569**	0.689**	0.428**	ns			
	K	ns	ns	ns	ns	ns		
	Cl	ns	ns	ns	ns	ns	0.790**	
	S	ns	ns	ns	ns	ns	0.501**	0.523**

Significance: * $P \leq 0.05$, ** $P \leq 0.01$, ns no significant.

Figure captions

Fig. 1 (a) Protocol for inducing Fe deficiency and carrying out Fe re-supply in GF 677 plants. (b) Labeling of leaves in GF 677 plants. Leaves 1 to 4 and 5 to 11 were expanded and basal leaves, respectively, at the start of the re-supply experiment. Leaves 0 to -4 (only 0, -1 and -2 shown in the graph) were leaves developed during the seven-day re-supply period.

Fig. 2 Leaf sections (3 x 3 mm) of control, Fe-sufficient (approximately 285 $\mu\text{mol Chl m}^{-2}$) and Fe-deficient (approximately 28 $\mu\text{mol Chl m}^{-2}$) leaves scanned by synchrotron radiation-induced X-ray fluorescence ($\mu\text{-SRXF}$).

Fig. 3 Two-dimensional Fe, Mn, Zn and Cu mapping in Fe-sufficient [+Fe] and Fe-deficient [-Fe] GF 677 leaves, obtained by synchrotron radiation-induced X-ray fluorescence ($\mu\text{-SRXF}$). Color indicates fluorescence intensity in relative units.

Fig. 4 Two-dimensional Ca, K, Cl and S mapping in Fe-sufficient [+Fe] and Fe-deficient [-Fe] GF 677 leaves, obtained by synchrotron radiation-induced X-ray fluorescence ($\mu\text{-SRXF}$). Color indicates fluorescence intensity in relative units.

Fig. 5 Chl concentration ($\mu\text{mol m}^{-2}$) of the different leaves along the stem of GF 677 plants growing in nutrient solutions containing 0 $\mu\text{M Fe(III)-EDTA [-Fe]}$, 90 $\mu\text{M Fe(III)-EDTA [+Fe]}$ or 180 $\mu\text{M Fe(III)-EDTA [180Fe]}$. Values shown were those found on day 7. Chlorophyll concentrations are shown for apical (0 to -4), expanded (1 to 4) and basal leaves (5 to 11). Data are means \pm SE of four replicates.

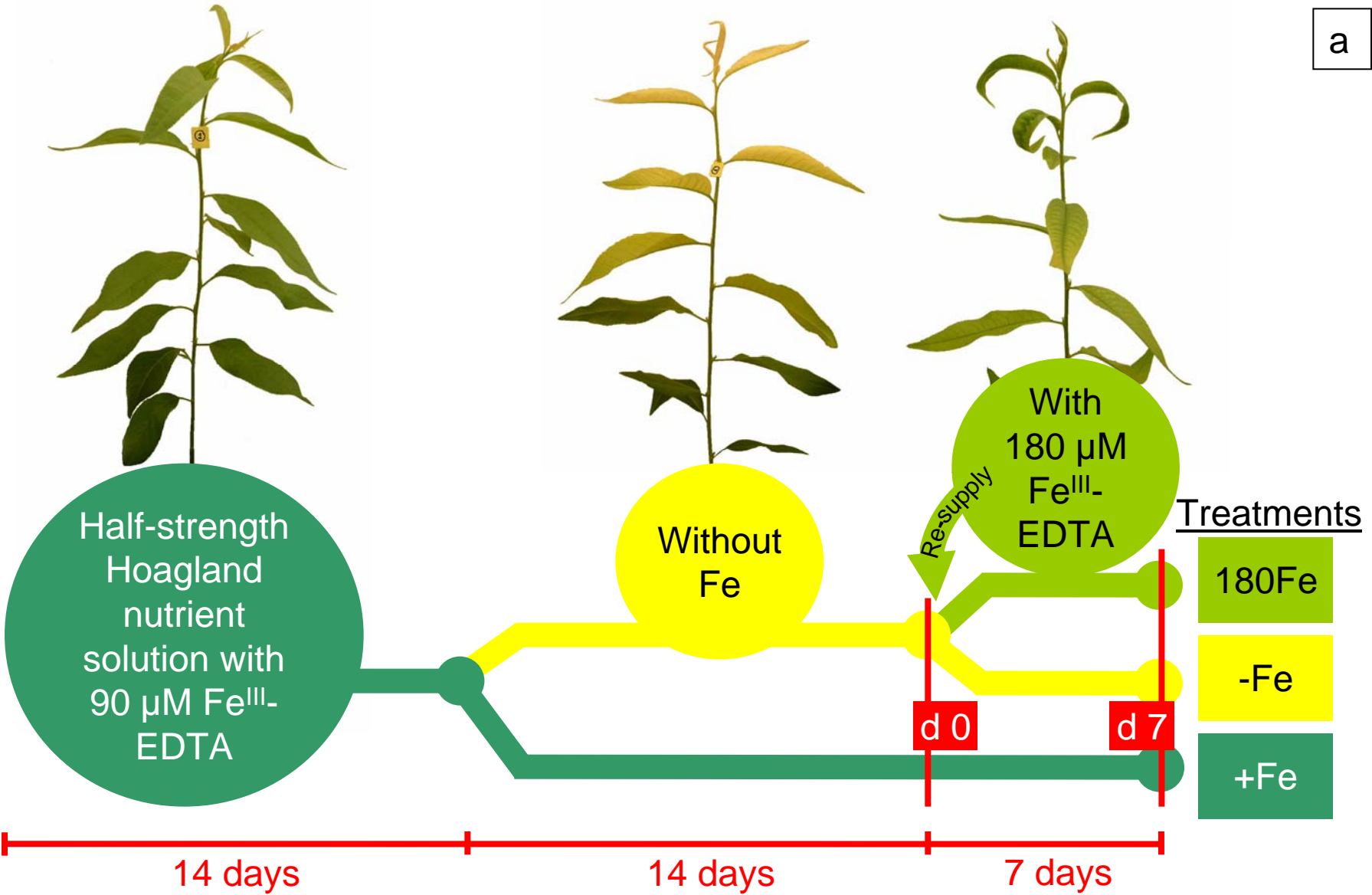
Fig. 6 Time course of the Fe concentration changes (in $\text{mg Fe kg}^{-1} \text{ DW}$) in different parts of GF 677 plants: apical, expanded and basal leaves, stems and roots, grown continuously with 0 $\mu\text{M [-Fe]}$ or 90 $\mu\text{M Fe(III)-EDTA [+Fe]}$, or without Fe for 14 days and then re-supplied with 180 $\mu\text{M Fe(III)-EDTA [180Fe]}$. Data were obtained at days 0, 4 and 7 for [-Fe]; days 0, 3 and 7 for [+Fe], and days 1 to 7 for the [180Fe] treatment, being 0 the day of Fe re-supply. Data are means \pm SE of three replicates, except for three of the apical samples for [180Fe] (d 1 to 3), where not enough material was available to run replicates.

571 Fig. 7 Relationships between mean Fe concentration (mg kg^{-1} DW) and mean
572 chlorophyll concentration ($\mu\text{mol m}^{-2}$) in apical (solid circles), expanded (open
573 circles), and basal (solid squares) leaves from GF 677 plants during Fe re-supply
574 (from day 0 to 7, ^{180}Fe). Arrows indicate the sequence of events for Fe and
575 chlorophyll concentration during Fe re-supply.

576 Fig. 8 Time course of the changes in root ferric chelate-reductase (FC-R) activity
577 ($\text{nmol Fe}^{2+} \text{ g}^{-1} \text{ FW min}^{-1}$) for whole GF 677 plants growing in nutrient solutions
578 containing 0 μM Fe(III)-EDTA [-Fe], 90 μM Fe(III)-EDTA [+Fe] or 180 μM Fe(III)-
579 EDTA [^{180}Fe]. Data were obtained at days 0, 4 and 7 for [-Fe]; days 0, 3 and 7 for
580 [+Fe], and days 1 to 7 for the [^{180}Fe] treatment, being 0 the day of Fe re-supply.
581 Data are means \pm SE of four replicates.

Figure 1a

a



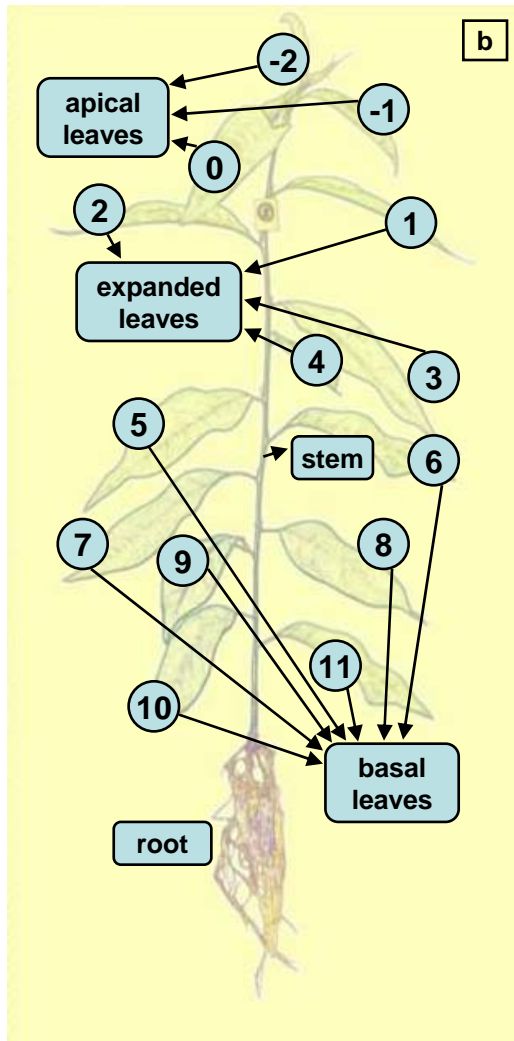


Figure 1b

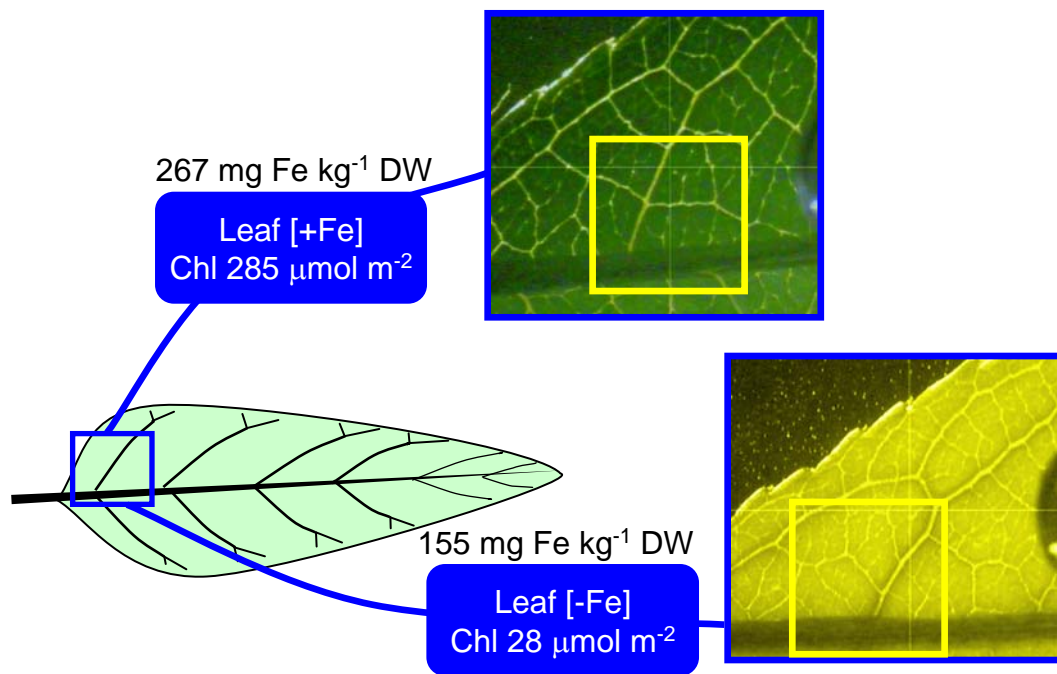


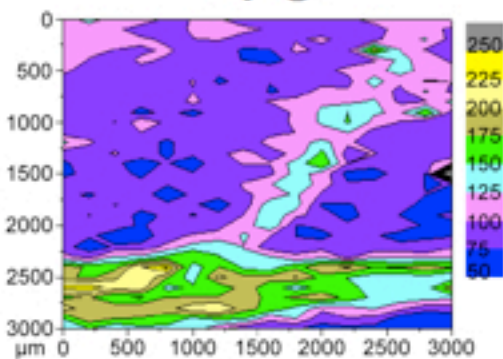
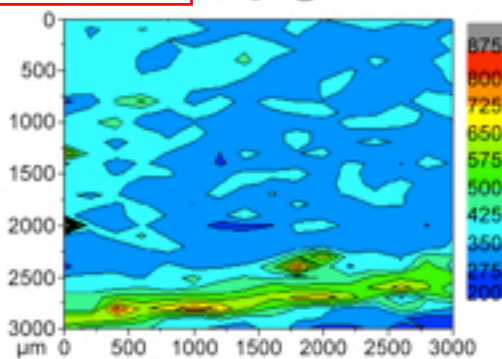
Figure 2

Figure 3

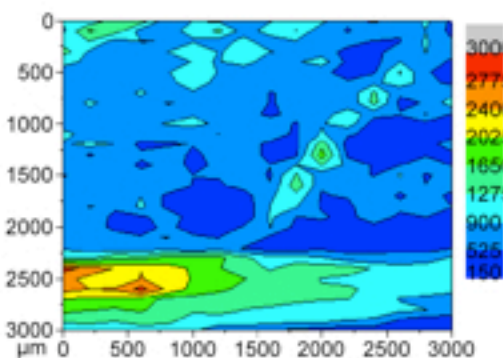
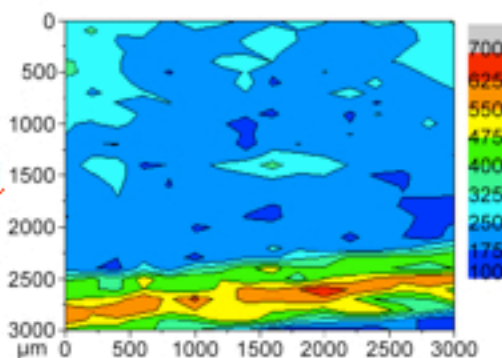
+Fe

-Fe

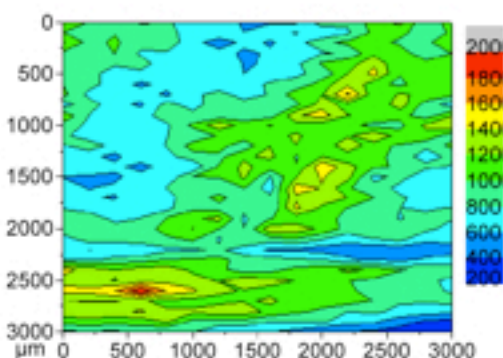
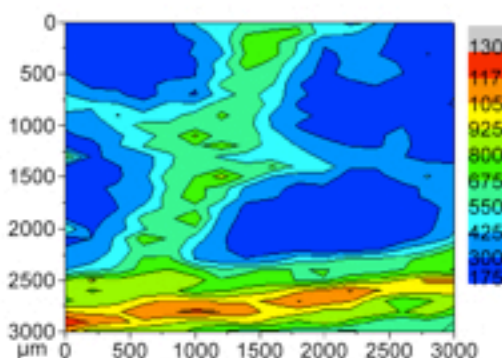
Fe



Mn



Zn



Cu

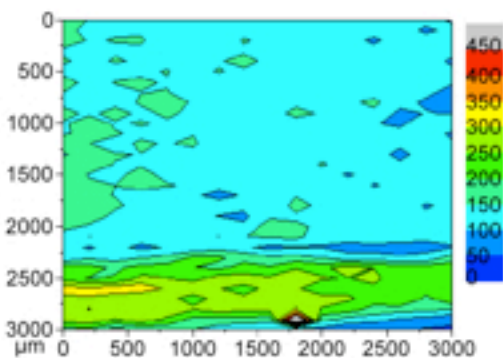
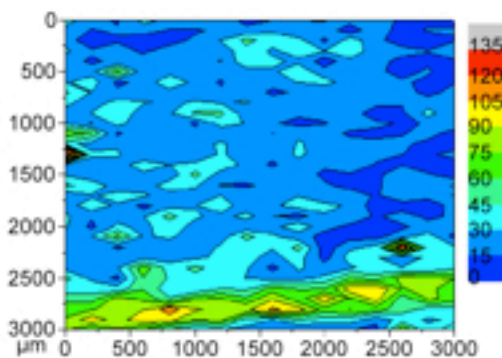
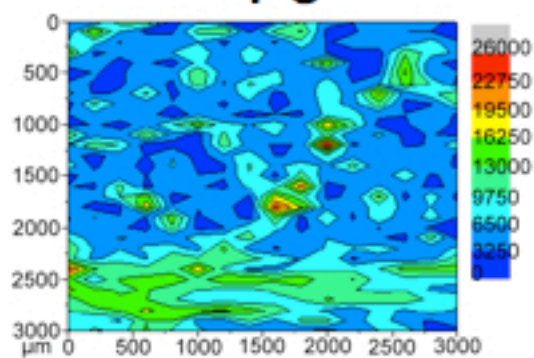
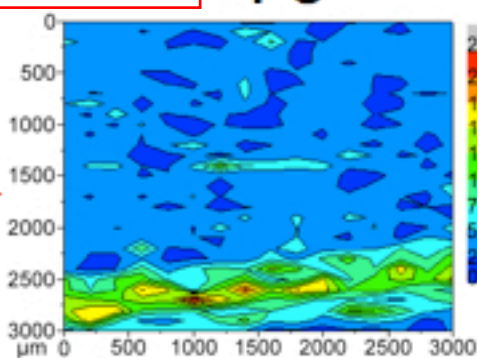
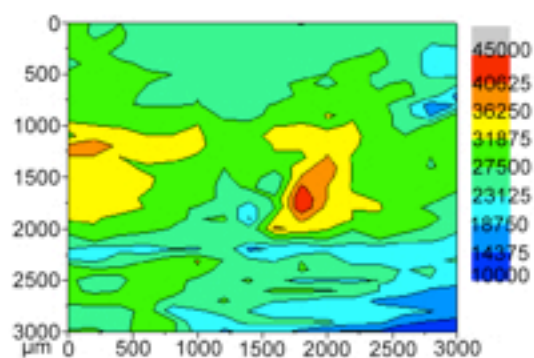
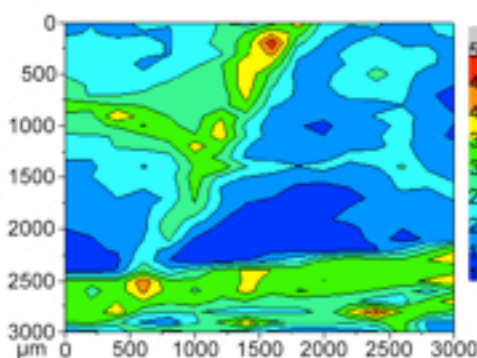
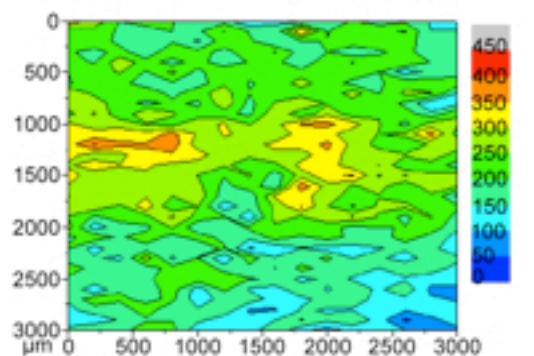
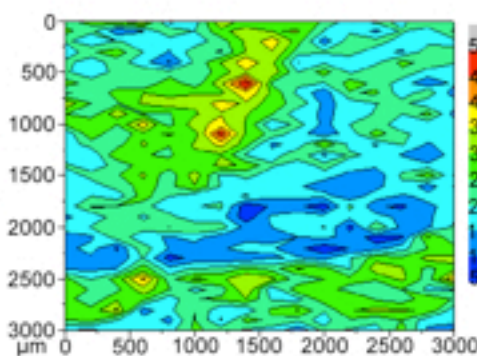
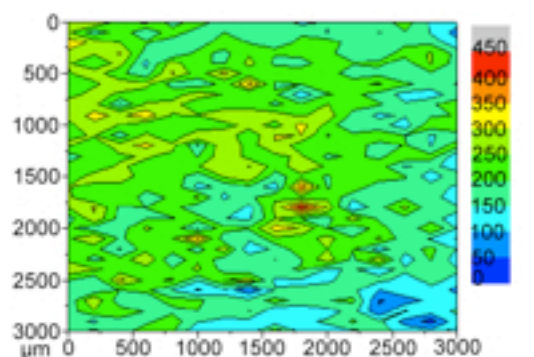
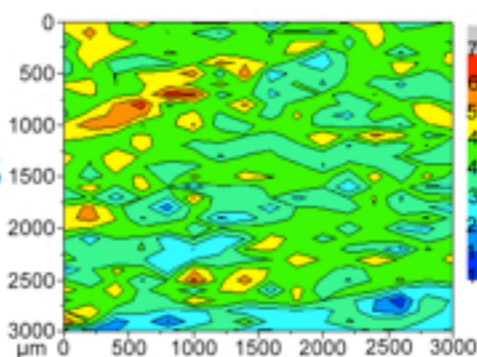


Figure 4

+Fe**-Fe****Ca****K****Cl****S**

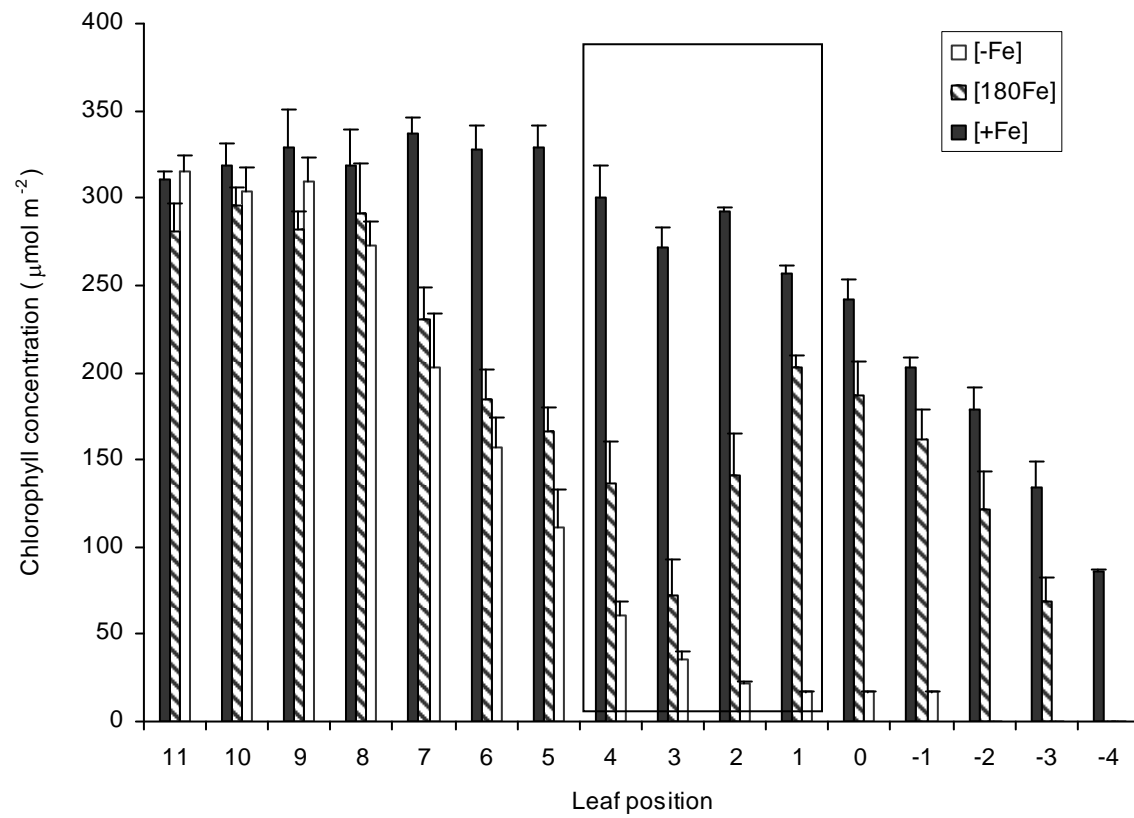


Figure 5

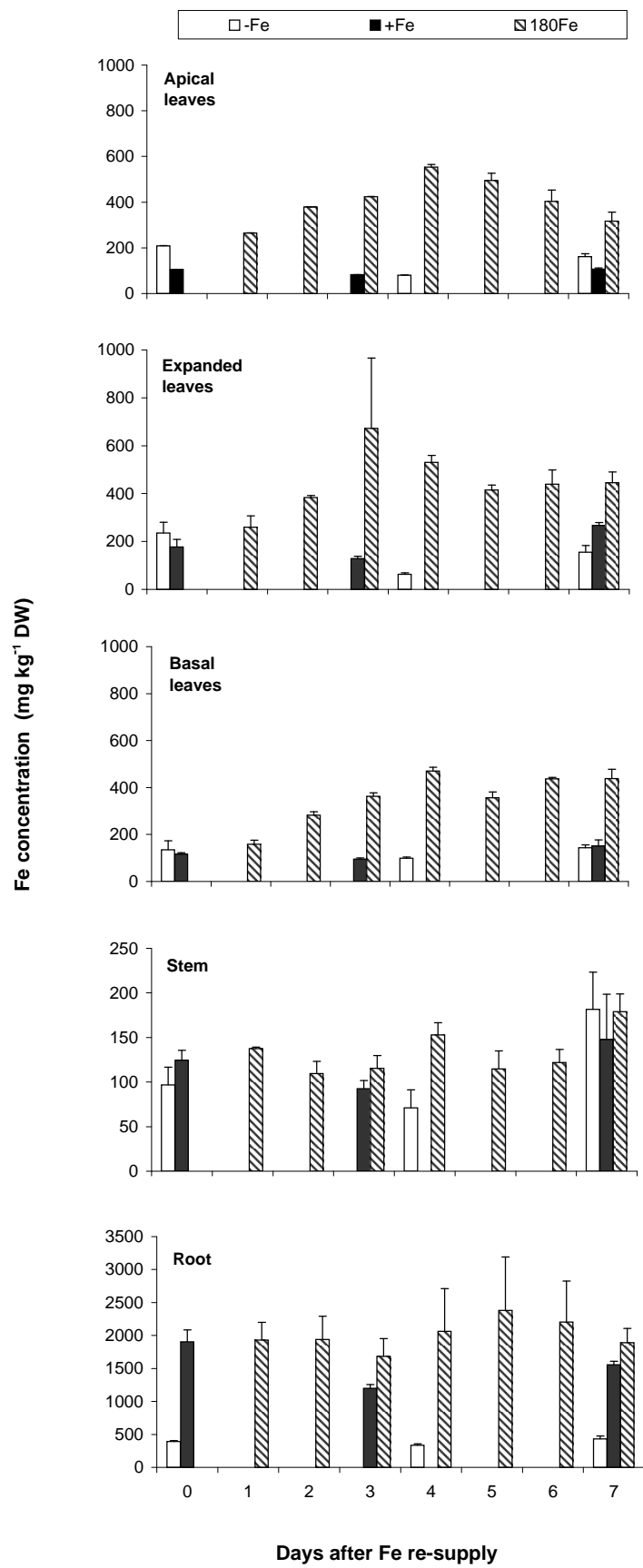


Figure 6

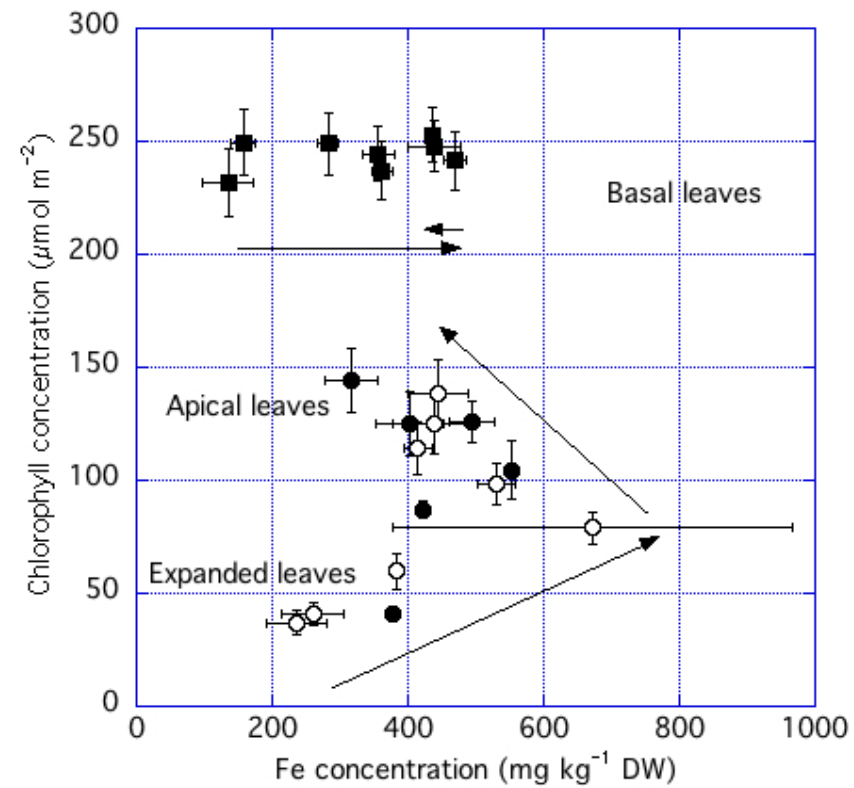


Figure 7

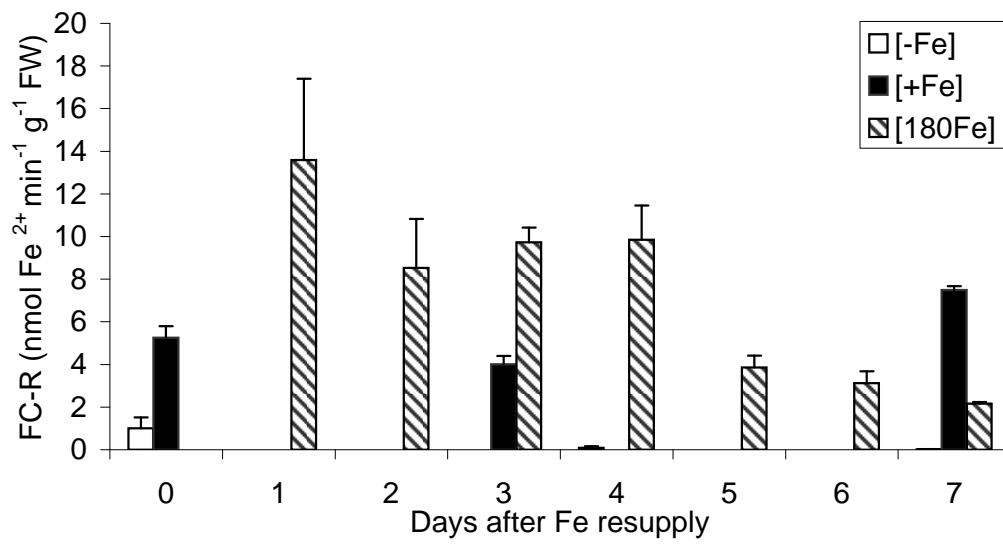


Figure 8